Domain growth and fluctuations during quenched transition to quark-gluon plasma in relativistic heavy-ion collisions

Ranjita K. Mohapatra* and Ajit M. Srivastava†
Institute of Physics, Sachivalaya Marg, Bhubaneswer 751005, India
(Received 25 March 2013; revised manuscript received 9 September 2013; published 2 October 2013)

We model the initial confinement-deconfinement transition in relativistic heavy-ion collisions as a rapid quench in view of expected rapid thermalization to a quark-gluon plasma state. The transition is studied using the Polyakov loop model, with the initial field configuration (in the confining phase) covering a small neighborhood of the confining vacuum $l \simeq 0$, as appropriate for $T < T_c$. Quench is implemented by evolving this initial configuration with the effective potential at a temperature $T > T_c$. We study the formation of $Z(3)$ domain structure and its evolution during the transition as l rolls down in different directions from the top of the central hill in the effective potential of l. When explicit $Z(3)$ symmetry-breaking effects (arising from dynamical quark effects) are small, then we find well defined $Z(3)$ domains, which coarsen in time. Remarkably, the magnitude plot of l shows vacuum bubblelike configurations arising during the quench. This first-order transitionlike behavior occurs even though there is no metastable vacuum separated by a barrier from the true vacuum for the parameter values used. When the initial field configuration everywhere rolls down roughly along the same direction (as will happen with large explicit symmetry breaking) then we do not find such bubblelike configurations. However, in this case we find huge oscillations of l with large length scales. We show that such large oscillations can lead to large fluctuations in the evolution of flow anisotropies compared to the equilibrium transition case.

DOI: 10.1103/PhysRevC.88.044901 PACS number(s): 25.75.−q, 12.38.Mh, 64.60.My

I. INTRODUCTION

In relativistic heavy-ion collision experiments (RHICEs) the collision of two nuclei leads to a hot dense region, which is expected to rapidly achieve a state of thermal equilibrium. For the relevant range of energies and colliding nuclei at RHIC and at LHC there is compelling evidence that a region of quark-gluon plasma is created in these collisions. Simulation results as well as experimental data, such as elliptic flow measurements, all point towards a very rapid thermalization to the quark-gluon plasma (QGP) phase, within a proper time less than 1 fm. We thus have a system that starts out in the confining phase, and within proper time of (probably much less than) 1 fm makes a transition to the QGP phase (with maximum temperature estimates ranging from 200 MeV to more than 700 MeV for the relevant energies in these experiments). Lattice results show that for real world QCD with small baryon density (as appropriate for the central rapidity regions in RHICEs) the transition is likely to be a crossover. With that, the dynamics of the transition depends crucially on the rate of temperature change compared to the time scale of the evolution of the order parameter field. For an equilibrium transition, we had studied the formation of $Z(3)$ domains and associated QGP strings using a first-order transition dynamics via bubble nucleation [1,2]. The transition was simulated using the Polyakov loop, $l(x)$, as an order parameter for the confinement-deconfinement transition [3]. These studies were appropriate for large chemical potential cases, as in lower-energy collisions, where the transition is expected to be of first order, though the results for $Z(3)$ wall network, etc., having certain universal characters, may be applicable in a more general context, even for a crossover, as explained in Refs. [1,2].

However, given the very short time scale of initial thermalization to QGP state, an equilibrium dynamics of the transition appears unlikely. Thermalization time even at RHIC energies is below 1 fm/c and it is expected to be much shorter at LHC energies. The thermalization time scale is related to the saturation scale Q_s in the color-glass condensate model and ranges from 0.6–1.0 fm [4], though much shorter thermalization time has also been discussed. For example, for RHIC, the value of thermalization time may be as short as 0.2 fm, see Ref. [5]. In view of the possibility of such short thermalization times, a more appropriate description of the transition should employ quenched dynamics in which the growth of $Z(3)$ domains will be via spinodal decomposition. In this paper we carry out such a study using the Polyakov loop, $l(x)$, as an order parameter for the confinement-deconfinement transition, with an effective potential of the kind used in Refs. [6–8]. For our simulation results we choose a definite parametrization of the effective potential [7] as was used in our previous works [1,2]. We model the phase transition in this Polyakov loop model, with the initial field configuration (in the confining phase) covering a small neighborhood of the confining vacuum $l \simeq 0$ as appropriate for the initial $T = 0$ system. In a quench, the temperature rapidly (rather suddenly) increases to its maximum value T_0 with the effective potential changed accordingly. The initial field l, unable to relax to the new equilibrium vacuum state in this short time, becomes unstable and rolls down in different directions from the top of the central hill in the effective potential of l. We study the formation of $Z(3)$ domain structure during this evolution. When explicit $Z(3)$ symmetry breaking effects (arising from dynamical quark effects) are small, then we find well defined

*ranjita@iopb.res.in
†ajit@iopb.res.in

 ©2013 American Physical Society

$Z(3)$ domains, which coarsen in time. With a symmetric initial patch of l, all the three $Z(3)$ domains form with random shapes and rapidly increase in size by coarsening. Remarkably, the magnitude plot of l shows vacuum bubblelike configurations, such as those that arise in a first-order transition, arising during the quench in this case (when the initial field rolls down in different directions). This first-order transitionlike behavior occurs even though there is no metastable vacuum separated by a barrier from the true vacuum for the parameter values used. These bubblelike configurations expand as well, somewhat in similar manner as during a first-order transition.

When the initial patch of l is only partially symmetric around $l = 0$ (as appropriate for small explicit symmetry breaking from quark effects), the dynamics retains these qualitative aspects with expected changes. Thus, true vacuum domains (with $\theta = 0$) are more abundant and they also grow fast at the cost of the other two $Z(3)$ domains (which are now metastable due to explicit symmetry breaking). Still, for small explicit symmetry breaking, all the three types of domains occur during the initial stages of the transition. There are few, small $Z(3)$ walls as there are fewer metastable $Z(3)$ domains embedded in the dominant true vacuum with $\theta = 0$. These walls shrink rapidly and eventually only the true vacuum survives.

The dynamics is found to be very different when the explicit symmetry breaking due to quark effects is taken to be strong. In this case the initial patch of l (around equilibrium point for $T = 0$ effective potential) could be significantly shifted towards the true vacuum for the quenched $T = T_0$ effective potential. In such a situation, l will roll down roughly along the same direction with angular variations becoming smaller during the roll down. In this case only $\theta = 0$ vacuum survives and no other $Z(3)$ domains are formed. Also, in this case we do not find bubblelike configurations. However, in this case we find huge oscillations of l with large length scales. This behavior is known from previous studies of the dynamics of scalar field in a quench [9] and is expected here when angular variations are small. The dynamics of field in such a case is dominated by large length scale coherent oscillations. It leads to novel scenarios of reheating via parametric resonance in the case of inflation in the early Universe [9]. In our case of RHICEs also it raises important questions about the possibility of parametric resonance and of novel modes of particle production from these large oscillations of l during the early stages of the transition. In the present work we explore another important effect of these large oscillations, on the evolution of flow anisotropies in RHICEs. As most of the flow anisotropies are expected to develop during first few fm of the QGP formation, it becomes an important question if the presence of large oscillations of l can affect the development of these flow anisotropies. As we will see, this indeed happens and these large oscillations lead to large fluctuations in flow anisotropy. (Though, these oscillations, and their effects, may not be as enhanced as discussed here when all dissipative effects are properly accounted for.)

We mention here that we do not discuss which of the cases discussed here (small, or large explicit symmetry breaking) may actually be realized in RHICEs. This is primarily because of a lack of understanding of the magnitude of the explicit symmetry-breaking term near $T = T_c$. (Some discussion of this has been provided in our earlier works [1,2].) Also, the spread of initial field configuration about confining vacuum plays a crucial role here and that in turn depends on details of pre-equilibration stage. A proper understanding (or modeling) of this stage and resulting estimate of the initial spread is essential before one can make more definitive statements about the dynamics of the transition. We hope to discuss these issues in future. Our main purpose here is to illustrate the possibility of very different types of dynamics of transition depending on the initial configuration. Our results show that in quenched dynamics, $Z(3)$ domains, and resulting $Z(3)$ domain walls, can last for any reasonable length of time only when explicit symmetry-breaking terms are very small. Otherwise, either different domains do not form at all, hence no $Z(3)$ walls are formed, or fewer metastable $Z(3)$ domains form embedded in most abundant true vacuum region. In the latter case resulting $Z(3)$ walls are smaller to begin with, and disappear quickly.

The importance of $Z(3)$ walls in RHICEs has been discussed by us in previous works, where we have also emphasized nontrivial scattering of quarks from $Z(3)$ walls. We have explored its consequences for cosmology as well as for RHICEs [1,2,10,11], including the possibility of CP violating scattering of quarks from $Z(3)$ walls leading to interesting observational implications [12]. Recently an interesting possibility has been discussed by Asakawa *et al.* in Ref. [13] where it is argued that scattering of partons from $Z(3)$ walls may account for small viscosity as well as large opacity of QGP. Our results for the formation of $Z(3)$ domains during quench (which are abundant only for small explicit symmetry-breaking cases) can be relevant for the studies in Ref. [13]. In this context we mention that smallest reasonable size $Z(3)$ domains [hence $Z(3)$ walls] we find are of order 1–2 fm at very early times, and at that stage the magnitude of the Polyakov loop order parameter l is very small, of order few percent of its vacuum expectation value. The quark scattering from $Z(3)$ walls is likely to be small for such a small magnitude of l [10–12]. By the time the magnitude of l becomes significant, domains coarsen to have large sizes, of order several fm. Thus, in the context of our model it appears difficult to form very small $Z(3)$ domains that still can scatter partons effectively (as needed in the study of Ref. [13]).

It is important to note that our results for domain growth and fluctuations for the quench case are dominated by the spinodal instabilities during the roll down of the field from the top of the hill of the effective potential. These instabilities arise primarily from the nature of the quench when the initial field configuration becomes unstable to exponential growth of long wavelength modes due to sudden change in the shape of the effective potential (the quench), and will be in general present even if the transition is a crossover. In this sense we believe that the qualitative aspects of our results have a wider applicability and are not crucially dependent on the specific form of the effective potential used here.

We briefly mention here that issues related to the physical meaning of $Z(3)$ domains, etc., have been discussed in the literature (see discussion of these in our earlier works [1,2] and we will not repeat it here). We only note that recent work of Deka *et al.* [14] has provided a support for the existence of these

metastable vacua from lattice. We also note that a simulation of spinodal decomposition in the Polyakov loop model has been carried out in Ref. [15], where fluctuations in the Polyakov loop and growth of long wavelength modes (representing domain formation) are investigated. In comparison, the main focus of our work is on detailed growth of domains due to coarsening with and without explicit symmetry breaking, new bubblelike structures, and existence of large fluctuations affecting flow anisotropies in important ways.

The paper is organized in the following manner. In Sec. II, we discuss the essential aspects of the Polyakov loop model of confinement-deconfinement phase transition and the effective potential used from Ref. [7]. Section III presents the numerical technique of simulating the phase transition via quench. We first discuss the case without any explicit symmetry breaking and study the formation and evolution of $Z(3)$ domains during the quench. Section IV discusses the unexpected result of bubblelike structures arising during the quench. We also discuss the case of small explicit symmetry-breaking terms when true vacuum domains become more abundant, but the overall picture of the transition remains roughly similar. In Sec. V we discuss the case when explicit symmetry-breaking effects are strong leading to l rolling down everywhere roughly along $\theta = 0$. This leads to large oscillations of l. In Sec. VI we study the effects of these large oscillations on flow anisotropy and show that it leads to large fluctuations in elliptic flow and spatial eccentricity (as compared to the case of equilibrium transition). Section VII presents conclusions.

II. MODELING THE PHASE TRANSITION

We briefly recall the salient features of the model we use for the confinement-deconfinement phase transition. The order parameter is taken to be the expectation value of Polyakov loop $l(x)$,

$$l(\vec{x}) = \frac{1}{N}\mathrm{Tr}\left\{\mathcal{P}\exp\left[ig\int_0^\beta A_0(\vec{x},\tau)d\tau\right]\right\}, \tag{1}$$

where $A_0(\vec{x},\tau)$ is the time component of the vector potential $A_\mu(\vec{x},\tau) = A^a_\mu(\vec{x},\tau)T^a$, T^a are the generators of SU(N) in the fundamental representation, $\mathcal{P}$ denotes path ordering in the Euclidean time τ, g is the gauge coupling, and $\beta = 1/T$ with T being the temperature. N (=3 for QCD) is the number of colors. The complex scalar field $l(\vec{x})$ transforms under the global $Z(N)$ (center) symmetry transformation as

$$l(\vec{x}) \to \exp(2\pi i n/N)l(\vec{x}), \quad n = 0, 1, \ldots, (N-1). \tag{2}$$

The expectation value of $l(x)$ is related to $e^{-\beta F}$ where F is the free energy of an infinitely heavy test quark. For temperatures below T_c, in the confined phase, the expectation value of the Polyakov loop is zero corresponding to the infinite free energy of an isolated test quark. [Hereafter, we will use the same notation $l(x)$ to denote the expectation value of the Polyakov loop.] Hence the $Z(N)$ symmetry is restored below T_c. $Z(N)$ symmetry is broken spontaneously above T_c where $l(x)$ is nonzero corresponding to the finite free energy of the test quark. Effective theory of the Polyakov loop has been proposed by several authors with various parameters fitted to reproduce lattice results for pure QCD [6–8]. We use the Polyakov loop effective theory proposed by Pisarski [7,8]. The effective Lagrangian density can be written as

$$L = \frac{N}{g^2}|\partial_\mu l|^2 T^2 - V(l), \tag{3}$$

where the effective potential $V(l)$ for the Polyakov loop, in case of pure gauge theory is given as

$$V(l) = \left(\frac{-b_2}{2}|l|^2 - \frac{b_3}{6}(l^3 + (l^*)^3) + \frac{1}{4}(|l|^2)^2\right)b_4T^4. \tag{4}$$

At low temperature where $l = 0$, the potential has only one minimum. As the temperature becomes higher than T_c the Polyakov loop develops a nonvanishing vacuum expectation value l_0, and the $\cos 3\theta$ term, coming from the $l^3 + l^{*3}$ term above leads to $Z(3)$ generated vacua. Now in the deconfined phase, for a small range of temperature above T_c, the $l = 0$ extremum becomes the local minimum (false vacuum) and a potential barrier exist between the local minimum and global minimum (true vacuum) of the potential. (However, the quench temperature used here is much higher than this range and there is no barrier present at such temperatures.)

The effects of dynamical quarks is included in terms of explicit breaking of the $Z(3)$ symmetry, which is represented in the effective potential by inclusion of a linear term in l [7,8,16]. The potential of Eq. (4) with the linear term becomes

$$V(l) = \left(-\frac{b_1}{2}(l + l^*) - \frac{b_2}{2}|l|^2 - \frac{b_3}{6}(l^3 + l^{*3}) + \frac{1}{4}(|l|^2)^2\right)b_4T^4. \tag{5}$$

Here coefficient b_1 measures the strength of explicit symmetry breaking. The coefficients b_1, b_2, b_3, and b_4 are dimensionless quantities. With $b_1 = 0$, other parameters b_2, b_3, and b_4 are fitted in Refs. [7,8] such that that the effective potential reproduces the thermodynamics of pure SU(3) gauge theory on lattice [16–18]. The values of various coefficients from Refs. [7,8] are the same as used in our previous works [1,2] (including discussions about explicit symmetry-breaking strength b_1) and we do not repeat that discussion here. (With those values of parameters, the transition temperature is taken to be $T_c = 182$ MeV.)

III. NUMERICAL SIMULATION

In this work, we carry out a $2+1$ dimensional field theoretic simulation of the dynamics of confinement-deconfinement transition in a quench. First we work within the framework of Bjorken's boost invariant longitudinal expansion model [19] (without any transverse expansion) for the central rapidity region in RHICEs. To model the quench, we take the initial field configuration to constitute a small patch around $l = 0$, which corresponds to the vacuum configuration for the confining phase. This is for the case of zero explicit symmetry breaking. We will discuss the case of explicit symmetry breaking later. We have taken the initial phase of l to vary randomly between 0 and 2π from one lattice site to the other, while the magnitude of l is taken to vary uniformly between 0 and ϵ. (We have also taken the initial magnitude to have a fixed value equal to ϵ and the results are similar.) The value of ϵ is taken

to be much smaller than the vacuum expectation value (VEV) of l at $T = T_0$ and results remain qualitatively the same for similar small values of ϵ. We report results for $\epsilon = 0.01$ times the VEV of l. We take the quench temperature $T_0 = 400$ MeV.

This initial field configuration, which represents the equilibrium field configuration of a system with $T < T_c$, is evolved using the effective potential with $T = T_0 > T_c$. This represents the transition dynamics of a quench. The field configuration is evolved by the time-dependent equation of motion in the Minkowski space [20]

$$\frac{\partial^2 l_j}{\partial \tau^2} + \frac{1}{\tau}\frac{\partial l_j}{\partial \tau} - \frac{\partial^2 l_j}{\partial x^2} - \frac{\partial^2 l_j}{\partial y^2} = -\frac{g^2}{2NT^2}\frac{\partial V(l)}{\partial l_j}; \quad j = 1, 2 \tag{6}$$

with $\frac{\partial l_j}{\partial \tau} = 0$ at $\tau = 0$ and $l = l_1 + il_2$. The temperature is taken to decrease starting with the value T_0 (at an initial time τ_0, which we take to be 1 fm in all the simulations) as $\tau^{-1/3}$ as appropriate for the longitudinal expansion model. We mention that later in Sec. V we will consider an isotropic geometry for the transverse dynamics of QGP as relevant for RHICEs. There we will also model nonzero transverse expansion and then the central temperature will decrease faster than $\tau^{-1/3}$. Here, we take a 2000×2000 square lattice with physical size 20 fm $\times$ 20 fm. We take this lattice as representing the transverse plane of the QGP formed in a central collision and consider the midrapidity region. The evolution of field was numerically implemented by a stabilized leapfrog algorithm of second-order accuracy both in space and in time with the second-order derivatives of l_i approximated by a diamond-shaped grid [1,2]. We evolve the field using the periodic, fixed, and free boundary conditions for the square lattice. Here we present the results with periodic boundary conditions. We use $\Delta x = 0.01$ fm for the present case; later on we use different values of Δx, as shown by the lattice size in the corresponding figures. We take $\Delta t = \Delta x/\sqrt{2}$ as well as $\Delta t = 0.9\Delta x/\sqrt{2}$ to satisfy the Courant stability criteria. The stability and accuracy of the simulation is checked using the conservation of energy during simulation. The total energy fluctuations remains few percent without any net increase or decrease of total energy in the absence of dissipative $\dot{l}$ term in Eq. (6).

We mention here that the only dissipative term in Eq. (6) arises from the longitudinal expansion. In addition there will be sources of dissipation. For example, the phase transition may create heat and particle production. The resulting dynamics, then, will have additional sources of dissipation in the relaxation of the order parameter to the confined phase. Any dissipation will lead to suppression of oscillations of the field. Thus, the presence of additional sources of dissipation [which are not included in Eq. (6)] may lead to modification in our results on large oscillations of l as discussed below.

First, we present results for the formation and evolution of $Z(3)$ domains. The initial field configuration in the neighborhood of $l = 0$ becomes unstable when evolved with the effective potential [Eq. (5)] with $T = T_0 = 400$ MeV (at $\tau = \tau_0 = 1$ fm). As l rolls down in different directions, settling in one of the three $Z(3)$ vacua, different $Z(3)$ domains form. This can be understood clearly from Fig. 1, which shows the plot of the effective potential (in MeV/fm^3) at $T = 190$ MeV,

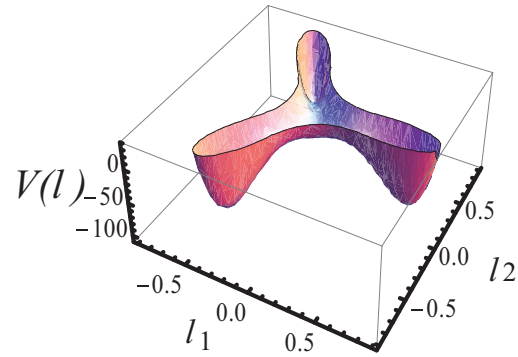

FIG. 1. (Color online) Plot of the effective potential V in units of MeV/fm^3 at $T = 190$ MeV.

and the three $Z(3)$ vacua. (We show the plot of V at $T = 190$ MeV to illustrate that at all temperatures $T > T_c = 182$ MeV, the three $Z(3)$ vacua are well formed.) Initially, as the phase of l is taken to vary randomly from one lattice site to the next, there are no well defined domains. Also, the magnitude of l is very small initially making any association of $Z(3)$ structure meaningless at such early stages. The situation remains similar for very early times as seen in Fig. 2(a) at an early stage $\tau = 1.2$ fm (i.e., 0.2 fm after the quench). In Fig. 2 we have shown the values of the phase of l around the three $Z(3)$ vacua in terms of different shades (colors) to focus on the evolution of $Z(3)$ domain structure. Thus all the values of the phase θ of l are separated in three ranges, between $-2\pi/6$ to $2\pi/6$ ($\theta = 0$ vacuum), between $2\pi/6$ to π ($\theta = 2\pi/3$ vacuum), and between π to $2\pi - 2\pi/6$ ($\theta = 4\pi/3$ vacuum). As the field magnitude grows, the angular variation of l also becomes less random over small length scales, leading to a sort of $Z(3)$ domain structure. $Z(3)$ domains become more well defined, and grow in size by coarsening as shown in sequence of Figs. 2(b)–2(d). Different shades (colors) in Fig. 2 represent the three $Z(3)$ domains. Figures 2(b)–2(d) show the growth of these domains at $\tau = 2.0$, 2.4, and 2.8 fm, as l relaxes to the three $Z(3)$ vacua and domains grow in size by coarsening. The magnitude of l is about 0.04, 0.08, 0.2, and 0.4 for Figs. 2(a)–2(d), respectively. Note that domains grow rapidly to size of order 2 fm within a time duration of about 1 fm as shown in Fig. 2(b). Within another 1 fm time, the domain size is about 4 fm as seen in Fig. 2(d).

The boundaries of different $Z(3)$ domains represent $Z(3)$ walls, and the junction of three different $Z(3)$ domains gives rise to the QGP strings. These objects have been discussed in detail in our earlier works [1,2,21].

We mention here that the smallest reasonable size $Z(3)$ domains [hence $Z(3)$ walls], which we find in our simulation are of order 1–2 fm at very early times, such as seen in Fig. 2(b). At this stage, the magnitude of the Polyakov loop order parameter l is still very small, of order few percent of its vacuum expectation value. This is important when one considers the possibility of nontrivial scattering of partons from $Z(3)$ walls [10–13]. The quark scattering from $Z(3)$ walls is likely to be small for such a small magnitude of l [10–12]. By the time the magnitude of l becomes significant, domains coarsen to have large sizes, of order several fm, as in Figs. 2(c) and 2(d)

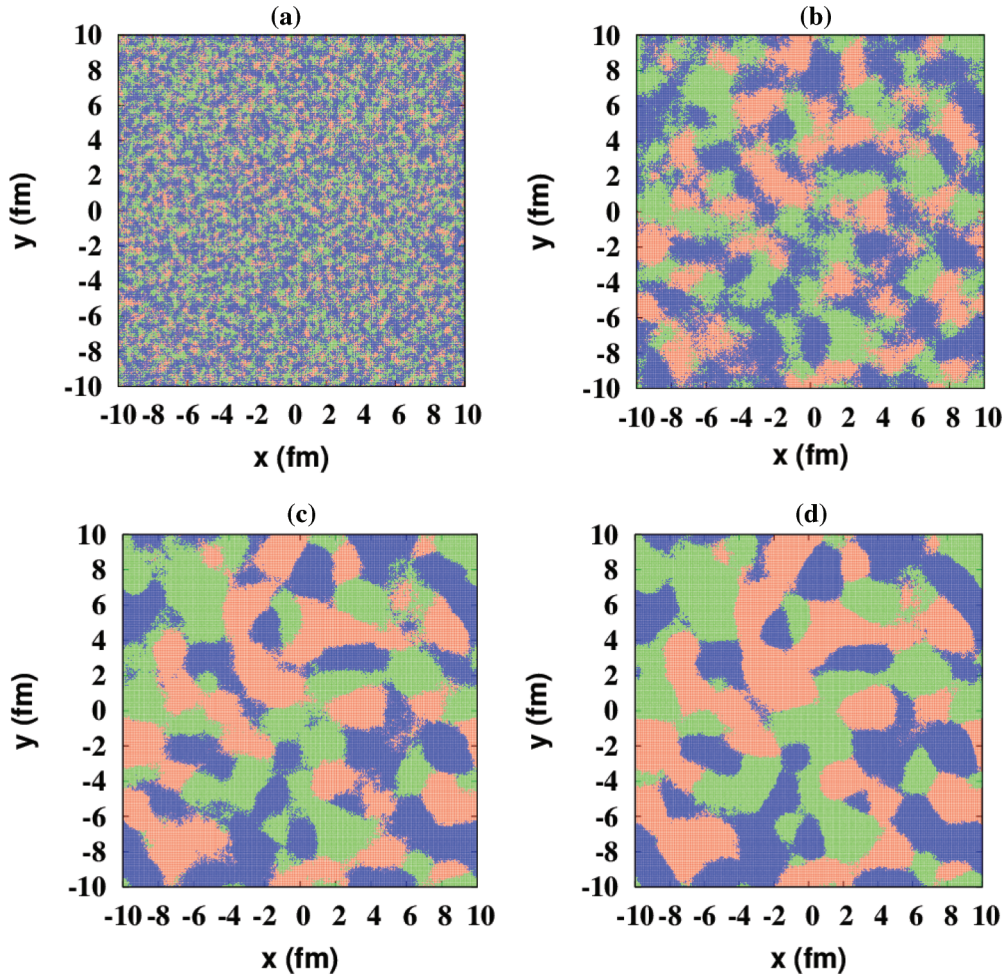

FIG. 2. (Color online) (a) Evolution of $Z(3)$ domain structure during a quench. Note that we take the initial temperature to be T_0 (=400 MeV) at proper time $\tau = \tau_0 = 1$ fm to set the initial conditions for the simulation. Different shades (colors) represent the three $Z(3)$ domains. (a)–(d) show the growth of these domains at $\tau = 1.2$, 2.0, 2.4, and 2.8 fm, (with corresponding values of temperature $T = 376$, 317, 298, 283 MeV) as l relaxes to the three $Z(3)$ vacua and domains grow in size by coarsening. The magnitude of l is about 0.04, 0.08, 0.2, and 0.4 for (a)–(d), respectively. Note that domains grow rapidly to size of order 2 fm within a time duration of about 1 fm as shown in (b). Within another 1 fm time, domain size is about 4 fm [as seen in (d)].

where the magnitude of l is about 20% and 40%, respectively, of its vacuum expectation value. Thus, in the context of our model, with quenched dynamics of transition, it appears difficult to form very small $Z(3)$ domains, which still can scatter partons effectively (as needed in the study of Ref. [13]).

IV. BUBBLELIKE STRUCTURES DURING QUENCH

In this section we show a very unexpected result. Figure 3 shows the sequence of plots of the magnitude of l during the quench described in the previous section. We note the appearance of bubblelike structures. These structures are also seen to grow in a manner similar to the bubbles for a conventional first-order phase transition, as in Refs. [1,2]. However, the distribution of the phase of l does not show any specific local variation related to these bubblelike configurations. In a roughly uniform region of the phase these localized bubblelike configurations arise and expand. We show here the plots of l in Fig. 3 corresponding to the initial central temperature $T = T_0 = 500$ MeV (at $\tau = \tau_0 = 1$ fm). The plots in Figs. 3(a)–3(d) are for $\tau = 2.0$, 2.8, 3.0, and 3.3 fm respectively, with the corresponding values of the central temperature being $T =$ 395, 355, 345, 336 MeV. It is important to note that at such high temperatures there is no metastable confining vacuum at $l = 0$ in the effective potential [2]. (A metastable confining vacuum exists from $T = T_c = 182$ MeV up to $T \simeq 250$ MeV.) There is no tunneling modeled (or thermal hopping over the barrier) here nor is it expected. One expects a simple roll down of the field representing the dynamics of spinodal decomposition during the quench. We mention that similar bubblelike configurations also arise with $T_0 = 400$ MeV. However, in that case the temperature range goes below $T = 250$ MeV. To make a clear case that these bubblelike configurations have nothing to do with a first-order transitionlike situation (even remotely), we have shown plots with $T_0 = 500$ MeV.

This result is very unexpected and points to new interesting possibilities for the phase transition dynamics. For example, such bubblelike structures may lead to a dynamics of phase

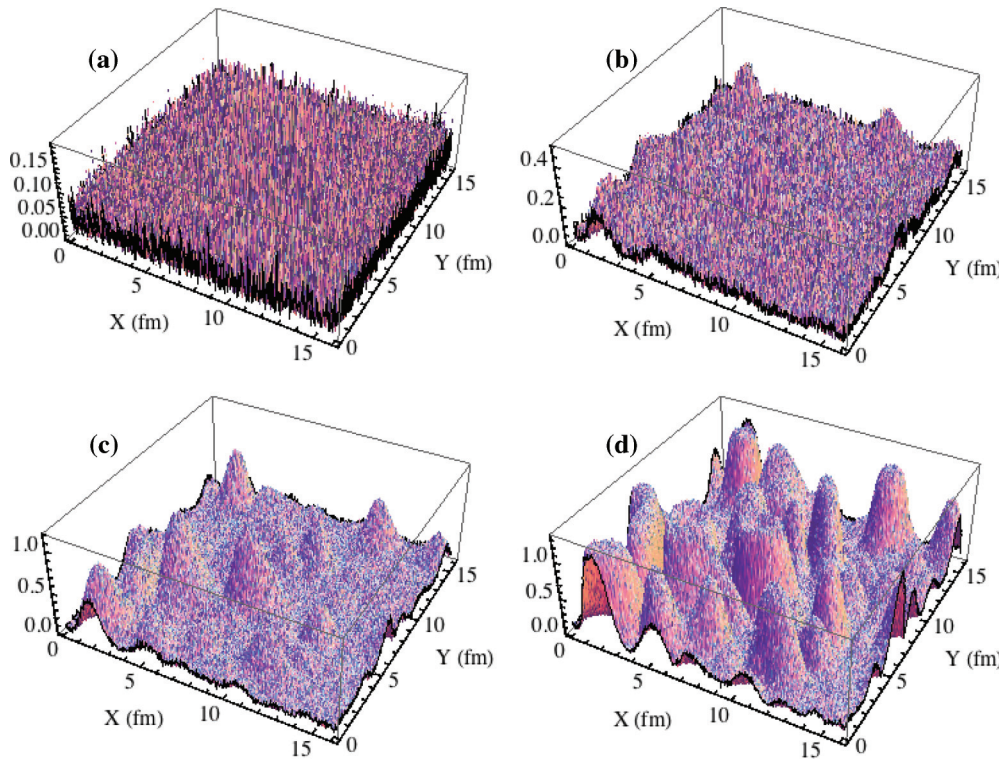

FIG. 3. (Color online) These plots correspond to initial central temperature $T_0 = 500$ MeV. (a)–(d) show the surface plots of $|l|$ during early stages with subsequent formation and growth of bubblelike structures just like a first-order phase transition. Plots in (a)–(d) are at $\tau = 2$, 2.78, 3, and 3.3 fm respectively, with corresponding temperature being $T = 395$, 355, 345, 336 MeV. These bubblelike configurations are surprising as there is no barrier here, and no metastable vacuum in the effective potential for this temperature range.

separation in the case of the universe similar to the original Witten's scenario [22], even when there is no underlying first-order transition. This may also have important implications for RHICEs. More importantly this new possibility of transition dynamics needs to be understood and analyzed in detail, see Ref. [23] for a study of these issues.

The studies of this section and the previous section apply to the case without any explicit symmetry breaking, i.e., with $b_1 = 0$ in Eq. (5). We have repeated these simulations with small explicit symmetry-breaking effects on the initial conditions. We take $b_1 = 0.005$ as in Ref. [2] here as well as in the next section. By small explicit symmetry-breaking effects on the initial conditions we mean that the initial patch of l is taken to shift towards $\theta = 0$ vacuum for $T = T_0$ effective potential, while still overlapping with the initial equilibrium value of l. The shift of the minimum at $l = 0$ to nonzero value of l is shown in the plot of the effective potential (for small values of l, in $\theta = 0$ direction) in Fig. 4. This small shift forces l to roll down to different θ directions at least at some fraction of lattice points, though a major fraction now rolls down towards $\theta = 0$. Figure 5 shows sequence of plots showing growth of $Z(3)$ domains in one such case. We see that one of the vacua ($\theta = 0$) expands dominantly while other domains remain relatively smaller. The $Z(3)$ domain walls in this case are smaller and disappear faster compared to the case without explicit symmetry breaking. The dynamics of bubblelike structure retains its qualitative aspects in this case as long as the field rolls down in different directions.

V. STRONG EXPLICIT SYMMETRY BREAKING AND LARGE FIELD OSCILLATIONS

Now we consider the case when explicit symmetry-breaking effects make the initial field configuration completely biased towards $\theta = 0$ direction. Here the initial patch of l rolls down entirely towards $\theta = 0$ direction with angular variations decreasing during the roll down. The dynamics of transition is entirely different in this case. Clearly there is no possibility of different $Z(3)$ domains here, hence no $Z(3)$ interfaces, or QGP strings will form. We also do not see any bubblelike structures

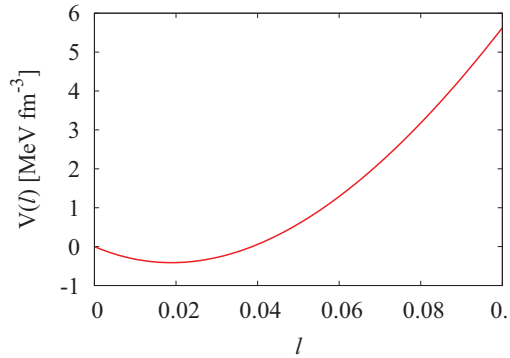

FIG. 4. (Color online) Plot of the effective potential V at $T = 190$ MeV in $\theta = 0$ direction for $b_1 = 0.005$. The minimum is shifted to nonzero value of l.

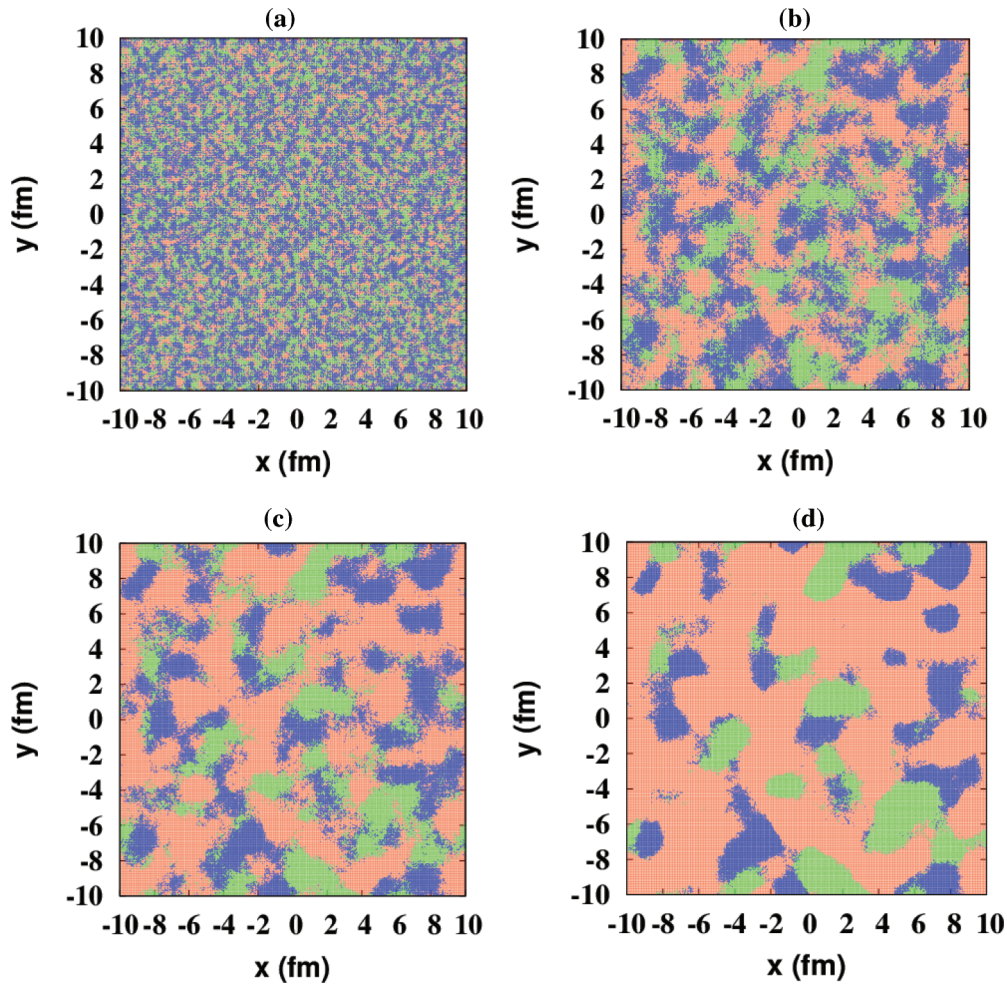

FIG. 5. (Color online) (a) Field configurations at different times with small explicit symmetry-breaking effects. The shading (color) representing the dominant region in (d) corresponds to the true vacuum with $\theta = 0$. (a)–(d) show the growth of domains for τ = 1.2, 1.6, 2.0, and 2.4 fm (with corresponding values of temperature T = 376, 342, 317, 298 MeV).

here as were seen in Fig. 3. Instead we find the l settles down to the true vacuum after undergoing huge oscillations, with large length and time scales.

These large oscillations are very similar to coherent oscillations of the inflaton field in the context of inflation in the early Universe [9]. For the inflation, the decay of such coherently oscillating field to particles can be via parametric resonance leading to novel features in the reheating of the Universe after inflation. The existence of similar oscillations here raises possibilities of parametric resonance for RHICEs and similar novel dynamics of particle production during such early stages of QGP evolution. As for the universe, new possibilities of thermalization and symmetry changes may arise here. We hope to explore these issues in a future work.

A direct implication of the existence of such huge oscillations of l in the context of RHICEs is its possible effects on the growth of flow anisotropies. In the hydrodynamical studies of elliptic flow in noncentral collisions it is known that much of the flow anisotropy develops during early stages of the plasma evolution [24,25]. In such studies one starts with the equilibrium QGP phase where flow develops due to pressure gradients. In view of the possibility of large oscillations during early stages of transition to the QGP phase, the equilibrium starting point of these hydrodynamics simulations becomes suspicious. Our present study does not allow us to address this issue in the context of hydrodynamical evolution. However, even with the field theoretical simulation in this work, we can do a comparative study of momentum anisotropy development with and without the presence of large oscillations of the order parameter field l. For this we proceed as follows.

First we need to model the initial QGP system with appropriate spatial anisotropies. One cannot then use the square lattice with uniform temperature. We use the temperature profile of Woods-Saxon shape with the size in the X and Y directions being different representing elliptical shape for a noncentral collision. This allows us to have a well defined size for the central QGP region, with temperature smoothly decreasing at the boundary of this region. The transverse size R of this system (i.e., profile of temperature) is taken to increase with uniform acceleration of 0.015 c per fm, starting from an initial value of R equal to the nuclear radius [25]. The initial transverse expansion velocity is taken to be zero. This expanding background of temperature profile is supposed to represent the hydrodynamically expanding quark-gluon

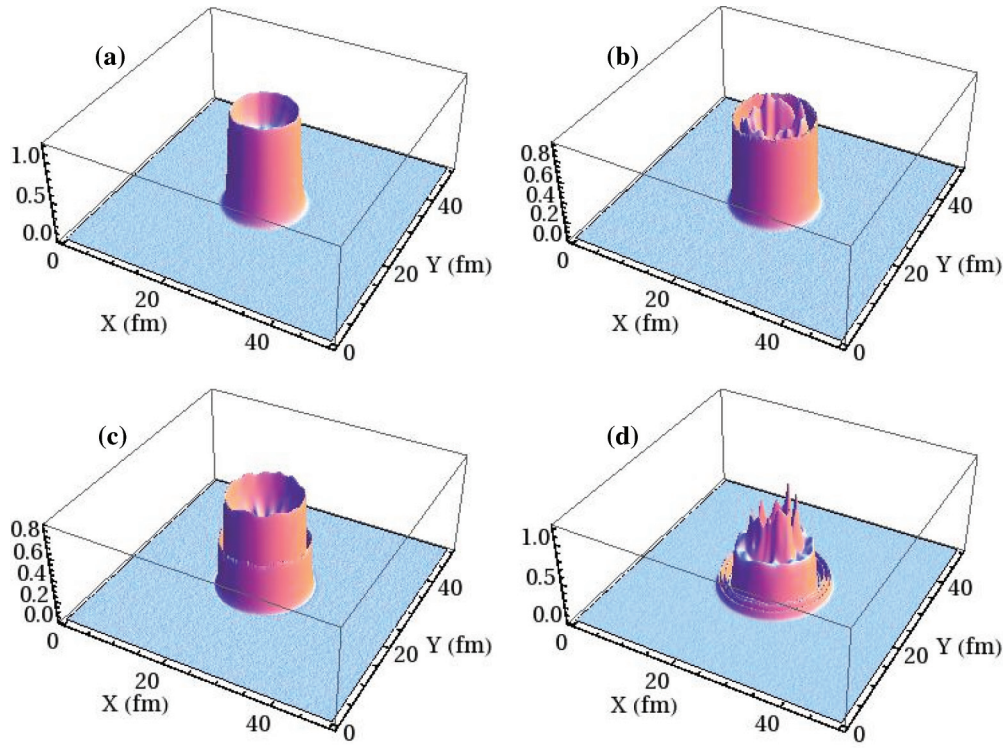

FIG. 6. (Color online) Surface plots of the magnitude of l with circular geometry for the QGP region. (a)–(d) show large oscillations of l during the quench when l rolls down everywhere towards the same vacuum with $\theta = 0$. Plots in (a)–(d) correspond to $\tau = 2.6$, 3.6, 4.4, 6.2 fm/c, with corresponding values of temperature being $T = 281$, 251, 228, 191 MeV, respectively

plasma in which the evolution of the order parameter field l will be studied. It may appear confusing as l is expected to represent the QGP phase. Indeed, the normalization of the effective potential in Eq. (5) from Refs. [7,8] is carried out precisely so that it represents energy density and pressure of gluons plus quark degrees of freedom. Still, the dynamics of l from Eq. (5) does not carry the information of hydrodynamical degrees of freedom. Various particle modes in l need to be excited, which should reach equilibrium, and only then we can expect some sort of hydrodynamical evolution. Clearly the initial field configurations assumed here are far from representing such a hydrodynamical state. A consistent interpretation of our simulation can be that we are studying long wavelength modes of l, which are coupled to a background of short wavelength modes, which are in thermal equilibrium. This equilibrated background is expanding with velocity as mentioned above, and drives the evolution of large wavelength modes of l via Eq. (6).

With this interpretation, our task is straightforward. The central temperature of the Woods-Saxon profile is taken to decrease by assuming that the total entropy (integrated in the transverse plane) decreases linearly as appropriate for Bjorken dynamics of longitudinal expansion. Note that, with the transverse expansion being nonzero now, the central temperature will decreases faster than $\tau^{-1/3}$. We show, in Fig. 6, a sequence of surface plots of the magnitude of l showing huge oscillations with large length scale during quench. Lattice here is again 2000×2000 but we take a large value of $\Delta x = 0.25$ fm so that the physical lattice size is 50 fm $\times$ 50 fm. The Woods-Saxon temperature profile (representing QGP region) is taken to have a diameter of about 16 fm as appropriate for Au-Au collision for RHICEs. The large physical size of the lattice allows for the evolution of the QGP region to be free from boundary effects.

At any stage we can calculate the energy momentum tensor $T^{\mu\nu}$ of l. We then calculate the spatial eccentricity ϵ_x of the l field configuration in the standard way,

$$\epsilon_x = \frac{\int dxdy(y^2 - x^2)\rho}{\int dxdy(y^2 + x^2)\rho}, \tag{7}$$

where ρ is the energy density. We can also calculate the momentum density at any time using T^{0x} and T^{0y}. Using these components we know the momentum density vector at every stage. By integrating it in angular bins we calculate its various Fourier coefficients, in particular the elliptic flow coefficient v_2.

VI. EFFECTS OF LARGE l OSCILLATIONS ON FLOW ANISOTROPY

To study the effects of large l oscillations on flow anisotropy, we consider two separate cases. Note that now we are considering the cases with explicit symmetry breaking, with its effect being strong on the initial field configuration. First we consider the quench case as described above. Here, we start with the initial field configuration corresponding to a small patch near the equilibrium point of $T = 0$ effective potential. The patch is taken, as above, with field magnitude

randomly varying in angle between 0 and 2π with random amplitude uniformly varying from 0 to 0.01 times the VEV of l but now shifted by a constant value of 0.011 times the VEV along $\theta = 0$ direction. This simulates the effect of strong explicit symmetry breaking as the entire patch rolls down towards $\theta = 0$ direction. This patch is then evolved with the temperature profile of Woods-Saxon shape as described above with the central temperature having initial value equal to $T_0 =$ 400 MeV. As a sample case we give results for the case when the initial (elliptical shaped) temperature profile has an eccentricity of 0.5 (with the major and minor axes being along the x and y axes respectively), which for uniform energy density will correspond to $\epsilon_x = -0.143$ from Eq. (7). The initial field configuration rolls down in the entire central region towards roughly $\theta = 0$ direction leading to strong l oscillations. ϵ_x, and flow coefficients, e.g., v_2 are calculated at each stage during the evolution. This is shown in Fig. 7. In this section we take the lattice to be 1000×1000 with the physical size of 25 fm $\times$ 25 fm. This still allows for sufficient separation of the QGP region (of size 16 fm diameter) from the boundary. Here we show plots (both for ϵ_x and for v_2) for two different realizations of the random initial field configuration (shown as solid and dashed plots). Here, and in all the figures below, we will show plots for a time up to $\tau = 10$ fm/c, starting with $\tau = \tau_0 = 1$ fm/c at the initial stage. The central temperature decreases (now faster than $\tau^{-1/3}$ due to nonzero transverse expansion) from an initial value $T = T_0 = 400$ MeV at $\tau = \tau_0 = 1$ fm/c to the final value $T = 147$ MeV at $\tau = 10$ fm/c. Note from the difference in solid and dashed plots in Fig. 7 that differences in the initial field configuration, which have very small magnitudes, lead to huge differences in the values of ϵ_x and v_2.

This situation should be compared to the case of equilibrium initial conditions, as appropriate for conventional hydrodynamical simulations. This equilibrium initial condition is implemented in the following manner here. For the initial temperature profile of Woods-Saxon shape (again, with a given eccentricity), with initial temperature $T = T_0 = 400$ MeV, we first need to determine the appropriate l configuration, which assumes a vacuum expectation value everywhere depending on the local value of the temperature. To achieve this, we first evolve the field configuration for 1000 time steps with highly

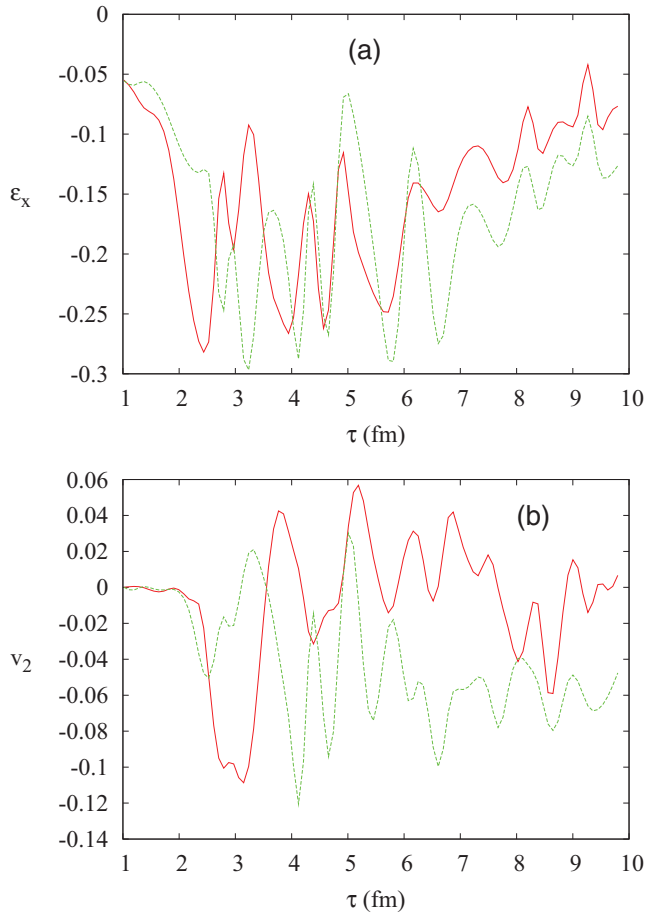

FIG. 7. (Color online) These plots correspond to the quench case when the initial elliptical shaped temperature profile has eccentricity of 0.5. Solid and dashed plots correspond to two different realizations of the initial random field configuration. (a) and (b) show plots for ϵ_x and elliptic flow v_2 respectively.

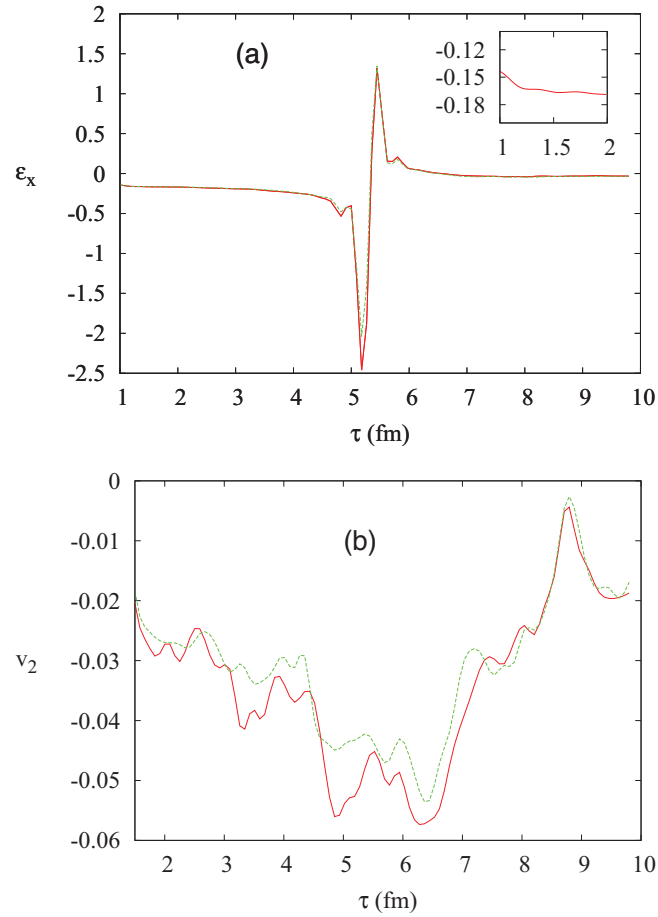

FIG. 8. (Color online) Plots as in Fig. 7, now for the equilibrium case. Solid and dashed plots show different realizations of the small random fluctuating part of the equilibrium field configuration. The temperature profile has same initial eccentricity of 0.5 (with corresponding value of $\epsilon_x = -0.143$) as in Fig. 7. (a) and (b) show plots of ϵ_x and elliptic flow v_2 respectively. Note, the initial value of ϵ_x for the equilibrated configuration in (a) is very close to -0.143 as shown by the plot in the inset.

dissipative dynamics while keeping the temperature profile to remain fixed at the initial profile. A reasonably smooth initial test profile of l is used as the initial field configuration. With highly dissipative evolution, the field everywhere settles to the local minimum of the potential quickly. The final configuration is found to be reasonably independent of the initial configuration assumed for l as long as it is smooth. This final configuration has correct profile as appropriate for the Woods-Saxon profile of temperature representing the lowest energy configuration everywhere. In order to make a suitable comparison with the quench case we must incorporate small fluctuations around this *equilibrium* configuration everywhere. For this purpose we add to the value of the field everywhere a small fluctuating field component with randomly varying angle between 0 and 2π and with random amplitude uniformly varying from 0 to 0.01 times the VEV of l (as for the quench case). This new field configuration represents the equilibrium field configuration everywhere, with small fluctuations. This is taken as the initial field configuration for subsequent evolution where now any extra dissipation is switched off. This stage is taken as representing the initial time $\tau = \tau_0 =$ 1 fm. The field now evolves with the field equations, Eq. (6). The temperature profile also is now allowed to change in time as mentioned above. ϵ_x, and v_2, etc. are calculated at each stage. Figure 8 shows these plots for this equilibrium case, starting from the time slightly after when extra dissipation (to achieve equilibrium configuration) has been switched off. When the random fluctuating component is introduced at every lattice site after the end of dissipative evolution, it introduces large gradients. Thus, for a very short time, there are large fluctuations as the field smoothes to certain level. Thus we show plots slightly after (by about 0.2 fm/c) the introduction of the random field component.

Comparison of Figs. 7 and 8 shows the dramatic effects of quench-induced oscillations on flow anisotropies. First note that for the equilibrium case the initial value of ϵ_x is close to the value -0.143 (as shown by the inset in Fig. 8), which exactly corresponds to the initial eccentricity of 0.5 for the temperature profile. This gives us confidence that our procedure of achieving equilibrated configuration works well. In contrast, the initial value of ϵ_x for the case of quench in Fig. 7 is very different showing the importance of fluctuations for this case. We further see huge fluctuations in the values of ϵ_x and v_2 in Fig. 7 compared to the equilibrium case shown in Fig. 8. Note that though there are oscillations in v_2 for the equilibrium case also, they do not change much from one event to another. In contrast, for the quench case in Fig. 7, there are huge variations between the two different realizations, i.e.,

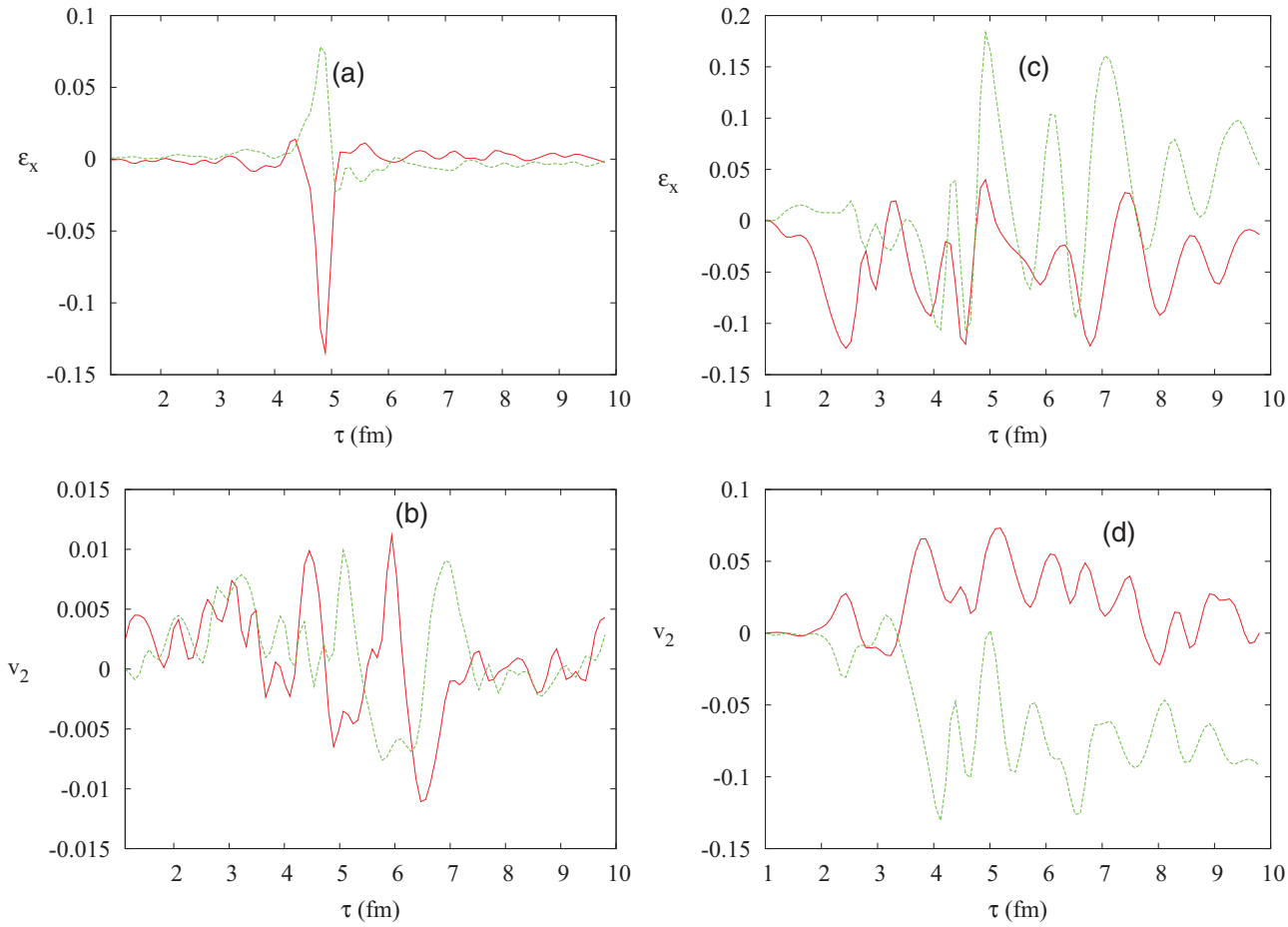

FIG. 9. (Color online) These plots are for the zero eccentricity for the temperature profile. In all the figures here, solid and dashed plots correspond to different realizations of initial random field configuration. (a) and (b) show plots of ϵ_x and v_2 for the equilibrium transition case, while (c) and (d) correspond to the quench case.

different events. These large fluctuations in Fig. 7 arise due to large oscillations in l, which itself depends on the nature of randomness in the initial field configuration. Note that plots for ϵ_x in Fig. 8 show a sharp change near $\tau = 5.5$ fm after which ϵ_x settles down to a value close to zero. The central temperature at that stage is about 208 MeV. Presumably a large part of the region (away from the central part where temperature is lower due to a Woods-Saxon profile) may be undergoing transition at that stage leading to large changes in field dynamics. We have checked with the contour plots that the ellipticity of the profile of l, as well as that of energy density, does not undergo rapid changes during this stage. (In fact this is a reflection of a shortcoming in our model where the temperature profile is taken to have definite initial eccentricity, and its further expansion is with definite acceleration as discussed above, starting with zero transverse velocity. A more appropriate model may be to take the time evolution of the spatial eccentricity of the temperature profile from hydrodynamical models and study the evolution of l using that.) We note strong fluctuations in both these quantities around this stage, which may be responsible for these large changes in ϵ_x at this stage. We hope to develop a better understanding of the dynamics during this stage, which is a topic for future work. At present what is important to note is that, apart from this peak region, everywhere else ϵ_x shows rather stable values settling down to a value close to zero after $\tau \simeq 5.5$ fm, and does not fluctuate much, as compared to the quench case in Fig. 7(a).

To further illustrate the importance of fluctuations for the quench case, we show plots for the case with zero eccentricity of the QGP region (i.e., for the temperature profile), which also will mean zero value of ϵ_x for uniform density case. Thus, any nonzero ϵ_x and v_2 arise only from the randomness in the initial field configuration. Figures 9(a) and 9(b) show the plots for the equilibrium case. We note that ϵ_x and v_2 remain very small, apart from a large change near $\tau = 5.5$ fm for ϵ_x, just as in Fig. 8. Again, at present what is important to note is that, apart from this peak region, everywhere else ϵ_x and v_2 remain very small for equilibrium case, as expected for the zero eccentricity case. Different plots in Figs. 9(a) and 9(b) correspond to different realizations of the initial random field configuration. This situation should be contrasted with the quenched case as shown in Figs. 9(c) and 9(d). Note that ϵ_x and v_2 now fluctuate with large amplitudes, even though eccentricity of the temperature profile is zero. Further, different realizations of the initial random field configurations lead to widely different plots of these quantities. This shows the fluctuating nature of development of flow anisotropies if large l fluctuations are present. These results suggest the dynamics of the order parameter field, especially such large length scale oscillations, may play an important role in determining flow anisotropies and it needs to be incorporated in the hydrodynamical models. (We emphasize again that with additional sources of dissipation present, large field oscillations and their effects will be suppressed.)

VII. CONCLUSIONS

We carry out a 2+1-dimensional simulation to study the dynamics of confinement-deconfinement transition as a quench for the central rapidity region in relativistic heavy-ion collision experiments. We work in the framework of the Polyakov loop model. The initial field (in the confining phase) is taken to cover a small neighborhood of the confining vacuum $l \simeq 0$ as appropriate for the initial $T = 0$ system. This initial field l, unable to relax to the new equilibrium vacuum state with quenched potential at $T = T_0 = 400$ MeV, becomes unstable and rolls down in different directions from the top of the central hill in the effective potential of l. We study the formation of $Z(3)$ domain structure during this evolution. When explicit $Z(3)$ symmetry-breaking effects (arising from dynamical quark effects) are small, then we find well defined $Z(3)$ domains, which coarsen in time. During early stages $Z(3)$ domains [and $Z(3)$ domain walls] have small sizes of order 1 fm. However at this stage the magnitude of l is very small, of order few percent of its vacuum expectation value. Domains coarsen rapidly as the magnitude of l grows and by the time $\tau = 4$–5 fm, domains are of size several fm. Surprisingly, the magnitude plot of l shows vacuum bubblelike configurations, such as those which arise in a first-order transition. This first-order transitionlike behavior occurs even though there is no metastable vacuum separated by a barrier from the true vacuum for the parameter values used. These bubblelike configurations expand as well, somewhat in a similar manner as during a first-order transition. This result points to new interesting possibilities for the phase transition dynamics. For example, such bubblelike structures may lead to a dynamics of phase separation in the case of the Universe similar to the original Witten's scenario [22], even when there is no underlying first-order transition. This may also have important implications for RHICEs. This new possibility of transition dynamics needs to be understood and analyzed in detail, see Ref. [23] for a study of these issues.

When the initial patch of l is only partially symmetric around $l = 0$ (as appropriate for small explicit symmetry breaking from quark effects), the dynamics retains these qualitative aspects, with true vacuum domains (with $\theta = 0$) growing dominantly at the cost of the other two metastable $Z(3)$ domains. In this case $Z(3)$ walls are fewer and relatively smaller, and they disappear more quickly. When the initial patch of l (around equilibrium point for $T = 0$ effective potential) is significantly shifted towards the true vacuum for the quenched $T = T_0$ effective potential (as will happen when explicit symmetry breaking is strong), then l rolls down roughly along the same direction with angular variations becoming smaller during the roll down. In this case only $\theta = 0$ vacuum survives and no other $Z(3)$ domains are formed. Also, in this case we do not find bubblelike configurations. However, in this case we find huge oscillations of l with large length scales. This is similar to the scenarios of reheating via parametric resonance in the case of inflation in the early Universe. In our case of RHICEs also it raises important questions about the possibility of novel modes of particle production from these large oscillations of l during the early stages of the transition. We have shown that these large l oscillations can strongly affect the evolution of flow anisotropies in RHICEs. The spatial eccentricity and the flow coefficients, e.g., the elliptic flow v_2 are found to undergo large fluctuations during the evolution of the system. These

results suggest the dynamics of the order parameter field, especially such large length scale oscillations may play an important role in determining flow anisotropies and it needs to be incorporated in the hydrodynamical models. Though we mention again that the dynamics of field studied here only incorporates the dissipative term arising from the longitudinal expansion. In general there will be additional sources of dissipation, e.g., from the phase transition dynamics leading to heat and particle production. This will affect the relaxation of the order parameter leading to suppression of oscillations of the field. Thus, the effects of oscillations discussed here (such as on flow fluctuations) may not be as enhanced as discussed in the present work. These additional dissipation effects are a topic for future research.

ACKNOWLEDGMENTS

We are extremely grateful to Umashankar Gupta for his help in the simulations, especially for the part involving novel bubblelike configurations. We are also very grateful to Rajeev Bhalerao, Vivek Tiwari, Sanatan Digal, P. S. Saumia, Abhishek Atreya, and Partha Bagchi for very useful comments and suggestions.

[1] U. S. Gupta, R. K. Mohapatra, A. M. Srivastava, and V. K. Tiwari, Phys. Rev. D **82**, 074020 (2010).
[2] U. S. Gupta, R. K. Mohapatra, A. M. Srivastava, and V. K. Tiwari, Phys. Rev. D **86**, 125016 (2012).
[3] L. D. McLerran and B. Svetitsky, Phys. Rev. D **24**, 450 (1981); B. Svetitsky, Phys. Rep. **132**, 1 (1986).
[4] J.-P. Blaizot, F. Gelis, J. Liao, L. McLerran, and R. Venugopalan, Nucl. Phys. A **873**, 68 (2012); D. Kharzeev, E. Levin, and K. Tuchin, Phys. Rev. C **75**, 044903 (2007).
[5] S. Pratt, Phys. Rev. Lett. **102**, 232301 (2009); P. Bozek and I. Wyskiel, Phys. Rev. C **79**, 044916 (2009).
[6] K. Fukushima, Phys. Lett. B **591**, 277 (2004); S. Rossner, C. Ratti, and W. Weise, Phys. Rev. D **75**, 034007 (2007).
[7] R. D. Pisarski, Phys. Rev. D **62**, 111501(R) (2000); in *Proceedings of the Meeting on Strong and Electroweak Matter SEWM2000, Marseille, France, June 13-17, 2000* (World Scientific, Singapore, 2001).
[8] A. Dumitru and R. D. Pisarski, Phys. Lett. B **504**, 282 (2001); Phys. Rev. D **66**, 096003 (2002); Nucl. Phys. A **698**, 444 (2002).
[9] J. H. Traschen and R. H. Brandenberger, Phys. Rev. D **42**, 2491 (1990); Y. Shtanov, J. Traschen, and R. Brandenberger, *ibid.* **51**, 5438 (1995); L. Kofman, A. Linde, and A. A. Starobinsky, *ibid.* **56**, 3258 (1997).
[10] B. Layek, A. P. Mishra, A. M. Srivastava, and V. K. Tiwari, Phys. Rev. D **73**, 103514 (2006).
[11] A. P. Mishra, A. M. Srivastava, and V. K. Tiwari, Indian J. Phys. B **85**, 1161 (2011).
[12] A. Atreya, A. M. Srivastava, and A. Sarkar, Phys. Rev. D **85**, 014009 (2012).
[13] M. Asakawa, S. A. Bass, and B. Muller, Phys. Rev. Lett. **110**, 202301 (2013).
[14] M. Deka, S. Digal, and A. P. Mishra, Phys. Rev. D **85**, 114505 (2012).
[15] A. Bazavov, B. A. Berg, and A. Dumitru, Phys. Rev. D **78**, 034024 (2008).
[16] A. Dumitru, D. Roder, and J. Ruppert, Phys. Rev. D **70**, 074001 (2004).
[17] O. Scavenius, A. Dumitru, and J. T. Lenaghan, Phys. Rev. C **66**, 034903 (2002).
[18] G. Boyd, J. Engels, F. Karsch, E. Laermann, C. Legeland, M. Lutgemeier, and B. Petersson, Nucl. Phys. B **469**, 419 (1996); M. Okamoto *et al.*, Phys. Rev. D **60**, 094510 (1999).
[19] J. D. Bjorken, Phys. Rev. D **27**, 140 (1983).
[20] T. C. Petersen and J. Randrup, Phys. Rev. C **61**, 024906 (2000).
[21] B. Layek, A. P. Mishra, and A. M. Srivastava, Phys. Rev. D **71**, 074015 (2005).
[22] E. Witten, Phys. Rev. D **30**, 272 (1984).
[23] S. Digal and R. K. Mohapatra (unpublished).
[24] J.-Y. Ollitrault, Eur. J. Phys. **29**, 275 (2008); R. S. Bhalerao, J. P. Blaizot, N. Borghini, and J.-Y. Ollitrault, Phys. Lett. B **627**, 49 (2005).
[25] P. F. Kolb, J. Sollfrank, and U. Heinz, Phys. Rev. C **62**, 054909 (2000).